Formation of graphene and hexagonal boron nitride on Rh(111) studied by in-situ scanning tunneling microscopy

Dong, G.

Chapter 6 Defects in the nanomesh lattice

6.1 Structure and formation of domain boundaries

All defect lines that we have encountered in the previous chapters on *h*-BN formation can be viewed as domain boundaries in the overlayer that derive from the problem to match the lattices of neighboring *h*-BN domains. These domains have nucleated independently in the early stages of the growth. The pre-seeding technique, where the initial nucleation had taken place during the warming up of the Rh surface after borazine exposure at room temperature, led to a wide distribution of domain orientations (see e.g. section 4.2). At a modest growth temperature of 865 K on such a pre-seeded surface, the *h*-BN domains could not reorient and the domain boundaries were mainly orientational misfit boundaries. On the atomic scale, the lattice cannot be continuous at such boundaries and unsaturated or hydrogen-terminated B- and N-atoms must be the consequence.

When the nanomesh structure was grown at 978 K, all domains were found to have the same orientation (within one degree). Even though orientational misfit boundaries cannot occur under these conditions, the nanomesh structure still exhibited defects lines at nearly all locations where growing *h*-BN patches encountered and merged. This is illustrated in Movie 3 [79] and in Fig. 6.1A-C. The reason for this is simply that the probability for any two islands to match, even when they have precisely the same orientation, is as low as 1/144. This is because each nanomesh unit cell covers 12 × 12 unit cells of the underlying Rh(111) surface, leading to 144 translational domains. A more detailed inspection showed that most defect lines appeared as a row of elongated,

compressed, and/or skewed nanomesh rings (Fig. 6.1D). This probably means that, in most cases, the islands attach to each other by forming a fully continuous, albeit somewhat distorted, *h*-BN network, without any dangling bonds. Like in any moiré pattern, the precise nanomesh period is very sensitive to small lattice distortions. For example, a local 4% stretching of the *h*-BN film would already be sufficient to double the size of a nanomesh unit. This effect makes the nanomesh pattern a highly efficient magnifying glass for modest variations in the lattice constant as shown in section 2.3.

In addition to the translational phase differences, we sometimes observed 180° misoriented islands, as had also been found for *h*-BN on Ni [24]. When such islands encountered properly oriented islands, strongly visible defect lines were introduced between them, probably involving dangling bonds in the *h*-BN lattice. This was to be expected, since a continuous network without dangling bonds would have required the formation of N-N bonds or B-B bonds.

In summary, the defects in a completely filled *h*-BN layer can be classified into three types: boundaries between two differently oriented domains, boundaries between domains of which one is 180° misoriented, and translational boundaries between domains with the same orientation. The first case only occurs when the *h*-BN domains originate from nuclei that are formed by warming up a Rh surface that is pre-exposed to borazine at a low temperature, such as room temperature. By necessity, orientational domain boundaries have dangling bonds, as is illustrated by the interrupted network in Fig. 6.1D. Also the boundaries between 180° misoriented domains come with a high density of dangling bonds. Translational boundaries between domains with the same orientation seem to avoid dangling bonds altogether and rather introduce elastic distortions in the overlayer lattice to accommodate the mismatch.

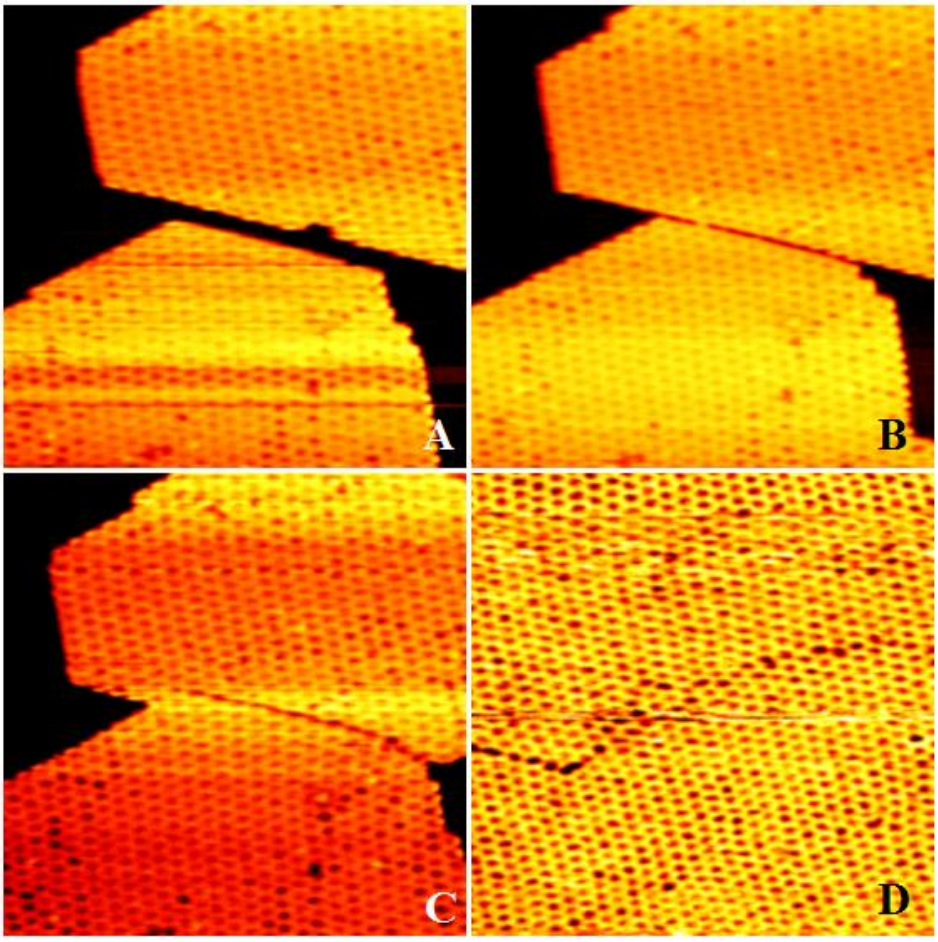

Fig. 6.1 (A-C) Three subsequent STM images from Movie 3 [79], which show the formation of a defect line in the *h*-BN nanomesh overlayer during growth in 1.2 $\times 10^{-9}$ mbar of borazine at 978 K. The two merging islands share the same orientation, but have a translational mismatch, which remains visible, after coalescence, as a row of deformed nanomesh unit cells. These lines were surprisingly immobile, as is illustrated in (D), which shows an STM image taken after the deposition had been completed and the fully *h*-BN covered Rh surface was heated further to 1135 K.
All images are 70 nm $\times$ 70 nm, and have been taken at $I_t = 0.05$ nA and $V_b = 1.2$ V (A-C) and 8.4 V (D), and at a rate of 1 image/52.5 s.

6.2 Removal of domain boundaries

Several experiments were performed to investigate whether the domain boundaries can be removed at high temperatures. As discussed in section 4.2 (Fig. 3.1C and D), the *h*-BN overlayer was capable of removing some of the shorter defect lines in the nanomesh structure. However, these domain boundaries were relatively short, typically not longer than one unit of the nanomesh lattice. Whether also longer domain boundaries could be removed was explored, using the network of orientational boundaries, shown in Fig. 4.2D, as a starting situation. In this experiment, the temperature was slowly ramped from 865 K to 1160 K. As shown in Fig. 6.2 and Fig. 6.3A, indeed the density of domain boundaries was reduced when the temperature was raised. In the process, the h-BN layer developed vacancy islands (Fig. 6.2B and C), which is the consequence of the area that has become available due to the removal of some of the domain boundaries (Fig. 6.2D), in particular those boundaries that separated *h*-BN domains with a large difference in orientation. The removal of domain boundaries and the clustering into vacancy islands of the area that is freed up in the process both require mobility inside the *h*-BN lattice.

From Fig. 6.3A, we can see that from 865 K where the layer was deposited to ~930 K the reduction of the domain boundary is modest. This is because the mobility of the inside the *h*-BN lattice is still low. From 1060 K to 1160 K the reduction was also low. This is because the low-angle domain boundaries remained immobile at much higher temperatures, even up to 1160 K, at which the *h*-BN layer began to disappear (desorb or dissolve). Similar STM observations were obtained when the sample of Fig. 6.1 was heated up, after the surface had been fully covered by *h*-BN at 978 K: all domain boundaries remained unchanged and static until the *h*-BN layer started to disappear at 1160 K. This absence of defect mobility is illustrated by Fig. 6.1D, which was recorded at 1135 K. Fig. 6.3B and C shows that the angle distribution of the moiré structure is wider at lower temperature. At 865 K the full width at half maximum (FWHM) of the Gauss fit is 23º (Fig. 6.3). A simple calculation of the moiré structure (see Chapter 2) shows that this angular width corresponds to a variation in orientation angle of the *h*-BN of no more than ±1º with respect to the Rh(111) substrate. With only one exception on a total of 70, all

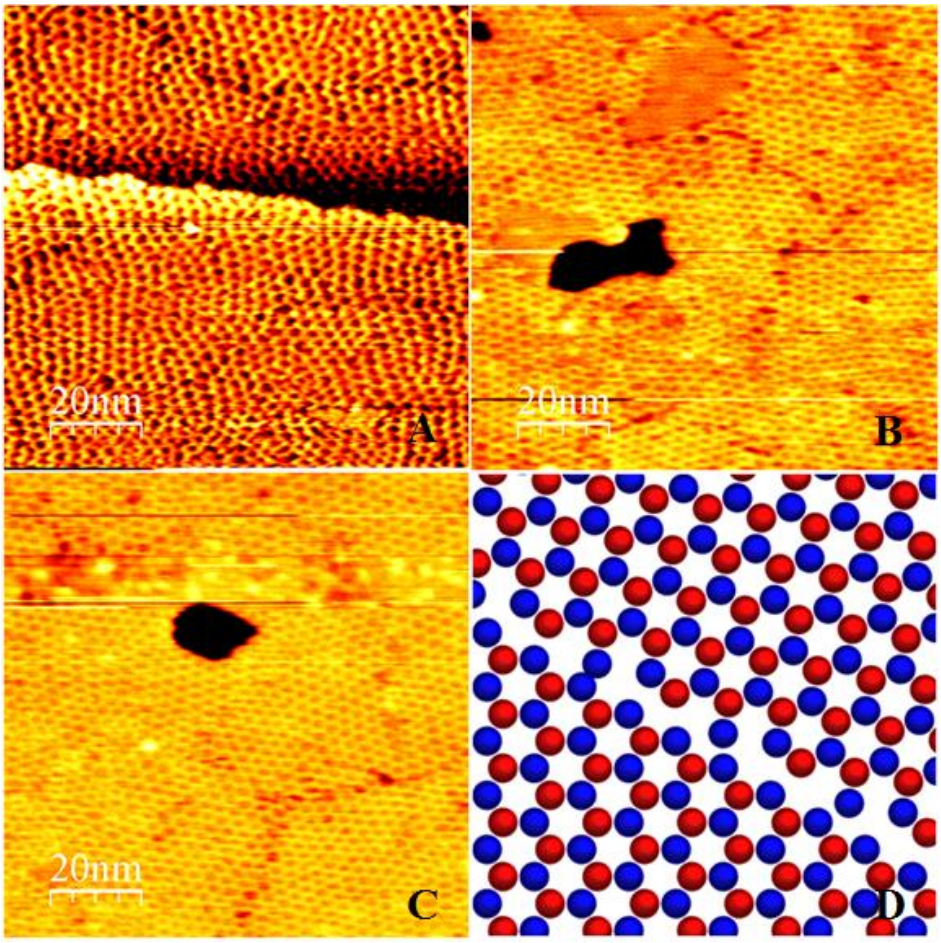

Fig. 6.2 (A - C) Three STM images taken while the sample shown in Fig. 4.2D was heated up. (A) Initial situation at the growth temperature of 865 K, with the surface fully covered by a heavily defective *h*-BN layer. (B) At 1050 K, the domains had become larger, and their orientations differed less from each other than at the lower temperature. The *h*-BN layer exhibited a certain density of vacancy islands. (C) At 1118 K, the domains had become even larger and the orientations had become more similar. Nevertheless, small-angle domain boundaries remained and they were stable until the *h*-BN layer disappeared at 1160 K. (D) Ball model of a high-angle (20 °) domain boundary between two *h*-BN patches. The blue and the red balls are the boron and the nitrogen atoms. In the boundary region, the local B and N densities are somewhat lower than in perfect *h*-BN. The vacancy islands in the *h*-BN layers in (C) and (D) are the material deficit that results from the removal of the high-angle boundaries.
All images are 100 nm × 100 nm and have been taken at I_t = 0.05 nA and V_b= -0.2 V, 6.7 V, 8.2 V for A – C, respectively.

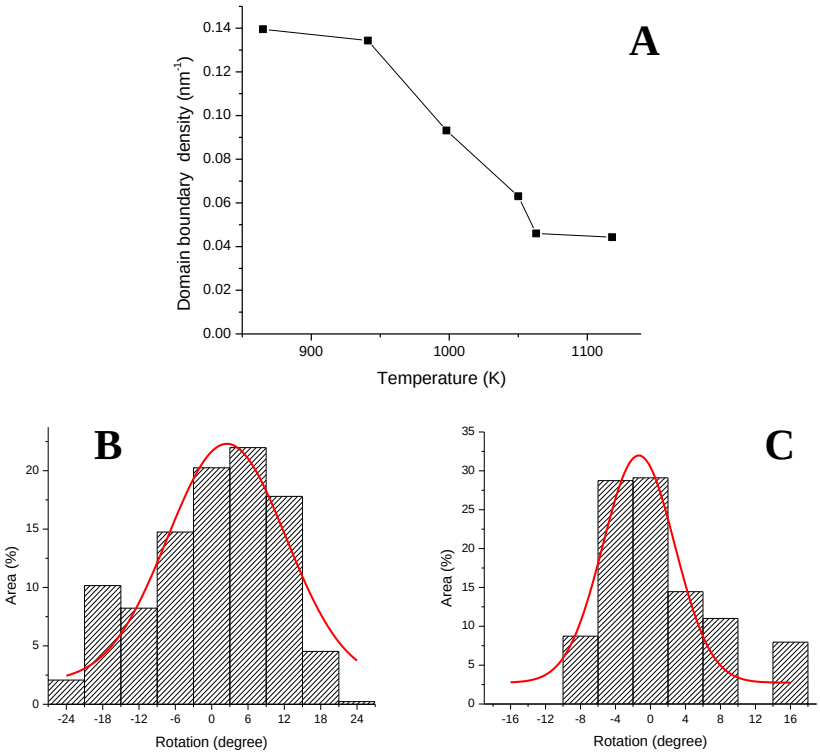

Fig. 6.3 (A) Temperature dependence of the domain boundary density, obtained from the experiment shown in Fig. 6.2. (B and C) Distributions of the rotation angle of the moiré structures observed at 864 K and 1118 K, respectively. Characteristic STM images at these two temperature are shown in Fig. 6.2. The full width at half maximum of the two Gauss fits are 23 º and 9.7 º for panel B and C, respectively. The asymmetry and offset with respect to 0 º were caused by a modest thermal drifting during the STM measurement.

domains were misoriented by less than 2º. At 1118 K, the FWHM of the moiré structure was 9.7º which corresponds a range of rotation angles of ±0.37º between *h*-BN and Rh(111). All domains in our STM images at this temperature were misoriented by less than 1.2º. These observations indicate that the mobility of the higher-angle domain boundaries is much higher than that of lower-angle grain boundaries. The large difference in mobility of high- and low-angle domain boundaries is very similar to that

observed for high- and low-angle grain boundaries in three-dimensional crystalline solids. Motion of a low-angle boundary is dictated by the discrete-dislocation character of the boundary structure and transport that therefore necessarily takes place in part along the boundary, whereas high-angle boundaries can move by transfer of atoms directly over the boundary [82, 83].

6.3 Conclusion

Our observations demonstrate that the structural quality of an *h*-BN nanomesh film cannot be improved by post-deposition treatments. At best the high-angle domain boundaries can be removed, but they are only formed when the *h*-BN is nucleated at low temperatures. As shown in Fig. 6.3, the post-deposition annealing temperature should be higher than 950 K to suppress the fraction of wrongly oriented domains. But even at temperatures higher than 1050 K the low-angle and translational boundaries cannot be removed, once formed. Thus, the defect lines remaining after deposition at temperatures above 950 K should be viewed as a fossil of the initial configuration of *h*-BN nuclei and their density directly reflects the nucleation density. To improve the quality of the film further, the only way is, therefore, to lower the density of such nuclei as much as possible. Nucleation-and-growth theory predicts that the nucleation density should be a function of the ratio *F/D*, where *F* is the flux of impinging borazine molecules, and *D* is the two-dimensional diffusion coefficient for these molecules (or their fragments) on the surface [84]. Therefore the best recipe is to combine a low flux and a high diffusion coefficient. It is for the latter reason (high *D*) that a high temperature is a prerequisite. When the diffusion length has become so high that the nucleation is dominated by defects in the Rh substrate, the *F/D* argument no longer applies and a further increase in temperature will not significantly improve the film quality. Possibly, this limiting situation has been reached at the typical growth temperature of 1050 K for *h*-BN nanomesh films on Rh(111).